IET Microwaves, Antennas & Propagation

Research Article

IET Journals
The Institution of Engineering and Technology

Coupling between coils in the presence of conducting medium

ISSN 1751-8725
Received on 22nd August 2017
Revised 17th July 2018
Accepted on 2nd August 2018
E-First on 9th November 2018
doi: 10.1049/iet-map.2018.5292
www.ietdl.org

Andrea Vallecchi[1] ✉, Son Chu[1], Laszlo Solymar[2], Christopher J. Stevens[1], Ekaterina Shamonina[1]

[1]*Department of Engineering Science, University of Oxford, Parks Road, Oxford OX1 3PJ, UK*
[2]*Department of Electrical and Electronic Engineering, Imperial College, London SW7 2BT, UK*
✉ *E-mail: andrea.vallecchi@eng.ox.ac.uk*

Abstract: The authors have studied analytically by simulation and by experiment the impact of a conducting medium on the mutual inductance between two coils, in particular as related to the attenuation of magneto-inductive (MI) waves. To illustrate the physics, the distributions of both the magnetic field and the Poynting vector are determined. They show that the plane wave approach used in the literature for the theoretical description of MI attenuation has only limited validity. It is further found that the mutual inductance becomes a complex quantity, its modulus declining monotonically as a function of conductivity or medium thickness. Their results will be relevant for the design and optimisation of MI waveguide links in conducting media, in general, and particularly when the attenuation is caused by soil conductivity. The results can also be useful for practical applications including *in vivo* communication and wireless power transfer for medical implants.

1 Introduction

It has been known ever since the work of Faraday and Oersted that currents flowing in a coil could produce a magnetic field and a time-varying magnetic field can induce currents in another coil – electromagnetic (EM) induction. This principle has led to many technologies including transformers, motors, generators and more recently near-field communications [1]. We have studied magneto-inductive (MI) waveguides in the past [2] exploiting this property for wideband communications and considered wireless power transfer via the same structures [3].

The wave aspect was first discussed 15 years ago [4, 5]. They were called MI waves. Their main merit is simplicity. They consist of a set of resonant coils mostly arranged in a linear array. They can be used at frequencies from the high kHz up to the low GHz region. The wave properties are usually derived from a model based on nearest neighbour interaction though higher-order interactions [5, 6] have also been studied and had to be implemented in a case when the length of a 100 element array was about five wavelengths [7]. When any distance is comparable with the wavelength, then, of course, the quasi-static approximations are no longer applicable and one must introduce retardation into the theory. Early experimental results were obtained in [8] followed by more detailed ones [9–12]. Various devices made up by MI waveguides were considered in [13].

Coming back to wireless communications, a review by Akyildiz and Stuntebeck [14] introduces the acronym WUSN standing for wireless underground sensor network. The emphasis is here on *underground*. That is the challenge the authors face. They investigate a solution by EM waves. In a later publication, Sun and Akyildiz [15] return to underground communications. They compare the EM wave solution with that of using MI waveguides and conclude that the MI solution is better because it does not need a large antenna (a small coil will do) and it does not suffer from multi-path interference. Further analyses by us [2, 16] and others [17, 18] included the investigation of noise properties as well. To increase the channel capacity, it was proposed in [19] to stagger the resonant frequencies of the elements. Digital signal transmission was considered in [20] and various optimisation techniques in [21]. An experimental study under realistic soil conditions was conducted in [22]. Underwater applications were discussed in [23, 24] and pipeline monitoring in [25].

Modelling of propagation of low-frequency waves in a lossy medium is also important in data links to embed biomedical systems and in body area networking for health-related applications since the human body and other biological tissues are moderately conductive at microwave frequencies. The range of conductivity is from about 0.05 S/m (fat) to about 1.5 S/m (blood). MI waves can also travel in the human body. Their main advantage in that context is their ability to prevent heating due to the excitation of standing waves on long conductors immersed in tissue [26], a well known problem when endoscopes are used in magnetic resonance imaging. The heating cannot occur in an MI waveguide since it is constituted by discrete elements. For realisations at 1.5 and 3 T, see [27, 28]. The achievable signal-to-noise ratio is studied in [29].

Similar physical processes have been investigated in the petroleum industry since the 1940s, where the aim was to find oil-bearing mud by means of low-frequency induction coils. The practise is known as induction logging. By measuring the transmission, particularly the phase of the arriving signal, between two or sometimes several coils placed in a bore hole, geologists were able to infer the conductivity of adjacent substrate that could reveal the presence of oil [30–33]. For a review, see [34].

An application suggested by Tesla [35, 36] at the beginning of the 20th century has become fashionable in the 21st century. It is near-field power transfer. Tesla wanted to provide all the energy needs of the world by wireless means. The aims are more modest nowadays. The main motivation for wireless transfer of power is the charging of the numerous electrical devices all of us have. We would like to mention a study of power transfer with the aid of a slab of metamaterial [37] and two further papers, where the transfer of power is based on MI lines and a solution is presented where the waveguide can be tapped at any point [3, 38].

We should recall one more direction of research in connection with coils and metal plates, and that is the shielding of coils. The first study analysing the means of shielding coils is that of Lewi [39] developed further by Smythe [40] and Foggo *et al.* [41]. All these studies give useful, though rather complicated, solutions. To our mind, the best analysis for the quasi-static case is that of Dodd and Deeds (D&Ds) [42], which gave the solution satisfying the boundary conditions in closed analytical form. This analysis has been more recently extended to predict the interaction of systems of coils in more general configurations and in the presence of layered conducting media [43–49].

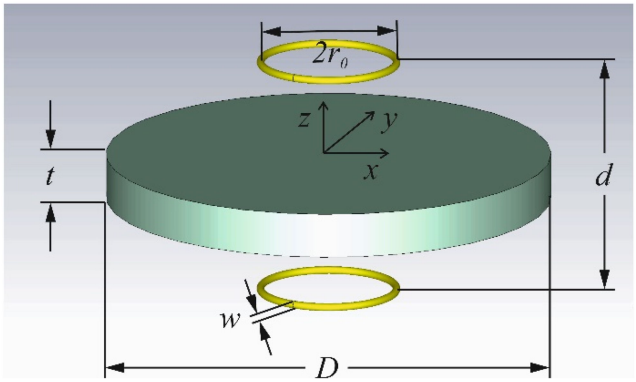

Fig. 1 *Schematic representation of two coils a distance d apart with a conducting block (thickness t and diameter D) between them*

The aim of the present paper is to investigate the impact of a conducting medium on the mutual inductance between two coils going beyond previous studies by including retardation into the equations, by using simulations and by going into the details of the physics. The basic configuration is simple. Some conductive material of thickness t and diameter D is inserted between two coaxial coils a distance d apart as shown in Fig. 1. In our paper, we shall cover the full range of conductivities from zero to that of copper, and the range of thicknesses from a thin plate to one filling the whole space between the coils.

We are primarily interested in the mutual inductance between the coils. In the absence of the conductive slab, the magnetic field distribution between two concentric coils can be found in practically every textbook on EM theory. When a conducting slab is introduced, the physics is still clear: a time-varying magnetic field generates eddy currents that create a magnetic field opposing the inducing field and lowering the coupling and hence the mutual inductance, or more precisely its real part, between the pair of coils. It is also obvious that an interference with the magnetic field of a transmitting coil will affect the phase of the magnetic field reaching the receiver coil. Since the induced EM force now has a phase shift relative to that one expects from simple, real mutual inductance. At the same time, eddy currents flowing in a conducting medium with finite conductivity also produce losses associated with the energy dissipated as heat in the material. Therefore, the overall interaction between two coils in the presence of a conducting medium can be generally described by a complex mutual inductance [49], or, in a completely equivalent manner – if M is a complex quantity, the associated impedance, Z_M, has indeed also a real part: $Z_M = \mathrm{j}\omega M = -\omega \mathrm{Im}(M) + \mathrm{j}\omega \mathrm{Re}(M)$– in terms of the coupling or mutual, impedance of the coils, as more commonly found [43–48].

Indeed mutual inductance can become a complex quantity also in another circumstance [7]. It occurs when the distance between the elements is not entirely negligible relative to the wavelength. In that case, the magnetic field excited by a transmitting coil has, beside the inductive, a radiating component as well. These two components will reach the next coil with different phases and amplitudes. The phase difference will then make the mutual inductance necessarily complex (note that the real part of the mutual inductance is often taken as positive or negative, but that only signifies the direction from which the magnetic flux reaches the coil). In fact, the real part may actually vanish. The complex mutual inductance between two coils in the presence of a conducting plate is discussed in a paper we published in a recent Conference Proceedings [50], which is only a preliminary and partial study preceding this one.

In Section 2, we shall first find the distribution of the magnetic field for a configuration showing both the penetration of the magnetic field and how the magnetic field lines can go round a finite conductive medium at higher conductivity. While most of our results are based on analytical models regarding the slab as being infinitely wide, we are able to have results for finite width plates as well by relying on simulations [51]. To elucidate the physical mechanism for the complex coupling, we determine the Poynting vector between the coils. We shall follow that by discussing methods relevant for the determination of the mutual inductance. The relationship between methods assuming the finite and infinite widths of the conducting medium is discussed. In Section 3, we present the mutual inductance, real part, imaginary part, modulus as a function of both conductivity and the thickness of the medium. Experiments and results are presented in Section 4. Conclusions are drawn in Section 5. In the Appendix, we present D&Ds' solution for the case of a single conducting slab in the air and including the effect of retardation.

2 Variation of the magnetic field and the Poynting vector

Fig. 2*a* (for $\sigma = 10$ S/m) and Fig. 2*b* (for $\sigma = 10^3$ S/m) show the results of finite elements calculation by Computer Simulation Technology Microwave Studio (CST MWS) allowing us to examine the polarisation of the magnetic field in the presence of the conducting medium. For simplicity and without loss of generality, due to the standard frequency scaling of EM phenomena, all results presented in the following are relevant to the sample angular frequency $\omega = 1 \times 10^9$ rad/s, i.e. $f = 159$ MHz; also, the coil configuration is kept the same throughout this paper: the radius of the coil is 11 mm, the cross-section of the coil has a diameter $w = 1$ mm, the separation between the two coaxial coils is 37 mm, the thickness of the cylindrical conducting block is 30 mm. The magnetic field generated by the transmitting coil is linearly polarised. In the presence of the conducting block, eddy currents are excited inside the conductor and produce a reaction field which can be significantly phase shifted with respect to the primary field. As a result, the total magnetic field, given by the superposition of the primary field of the transmitting coil and the reaction field generated by eddy currents, becomes elliptically polarised. Correspondingly the mutual inductance between the transmitting and receiving coils will become a complex quantity $M = 0.19\angle -110^\circ$. For the same block with conductivity $\sigma = 10^3$ S/m (Fig. 2*b*) the effect of eddy currents, stronger than in the previous case, is to make the normal component of the magnetic field at the bottom face of the block almost vanish, while the tangential component just outside the block is nearly doubled. In other words, the slab has become almost impermeable to magnetic fields and most of the magnetic field lines are deflected around the periphery of the block as one would expect for a perfect diamagnetic material. Unsurprisingly, the corresponding mutual inductance is considerably smaller than in the previous case: $M = 0.00018\angle -26^\circ$. The variation of the magnetic field due to the conducting block may be explained by primary and secondary fields that describe more precisely the physics of the phenomenon. Alternatively, we could simply say that the magnetic penetration is much reduced at higher conductivities due to the skin effect.

No study of EM phenomena is complete without looking at the movement of power, i.e. considering the Poynting vector moving from source to sink. For that, we need the solution of the full EM problem. In Figs. 3*a–d*, we show the magnitude (power flow density) and direction of the Poynting vector from the transmitting coil at the top, to the receiving coil at the bottom, for 22 mm diameter coils, 37 mm apart with a conductive block 30 mm thick between them, at a frequency of 159 MHz and for four different conductivities. In Fig. 3*a*, the case of coils in free space ($\sigma = 0$) is plotted as a reference. Even for the relatively small conductivity of $\sigma = 10$ S/m, considered in Fig. 3*b*, the conducting block introduces a significant attenuation of the power flowing between the two coils. As the conductivity further increases to 100 and 1000 S/m, the Poynting vector not only gets more and more attenuated, but its direction changes considerably as it is being diverted to be mostly perpendicular to the lateral surface of the block by the boundary conditions, there constraining the fields, in good consistency with the behaviour of the magnetic field that it showed in Fig. 2*b* going around the block. Thus, the physical picture given by the Poynting vector further corroborates that obtained by plotting the magnetic field lines. It is useful to note here that for the higher conductivities, there is still energy leaving the course and being absorbed by the eddy losses in the conducting block, but in a

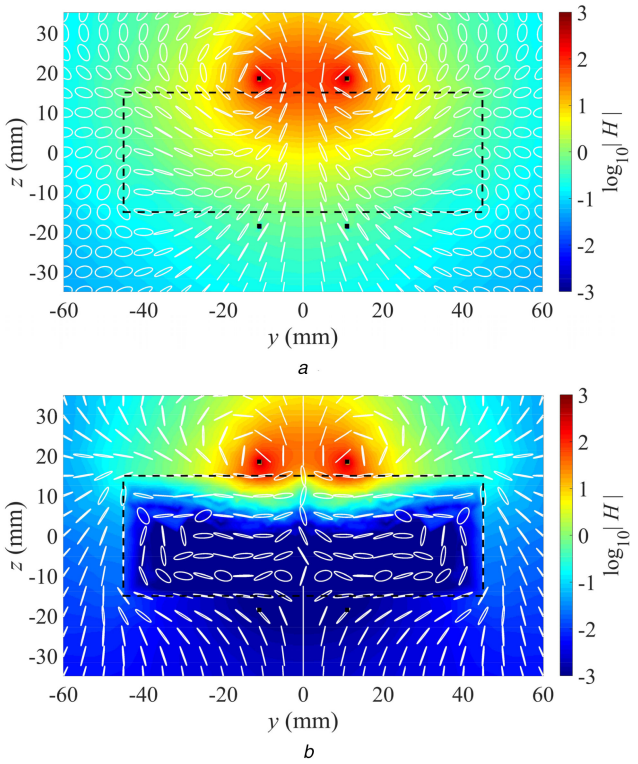

Fig. 2 *Polarisation ellipses and magnitude of the total magnetic field produced by a transmitter coil when a coaxial receiver coil displaced by 37 mm and a 30 mm thick conducting cylindrical block are present. Ellipse axes are normalised and plotted at a sampling step of 5 mm along the y and z directions. Black lines mark the cross-sections of the conducting block, and transmitter (top) and the receiver (bottom) coils. The conductivity of the block is*

(a) $\sigma = 10$ S/m; ***(b)*** $\sigma = 10^3$ S/m

gradually decreasing thickness at the surface, as one may expect from skin effect considerations.

It is quite clear that due to the conductivity of the block, the mutual inductance is considerably reduced. How can we determine this analytically? This is far from a trivial question. In many publications, among which [18, 22], it is suggested that it suffices to consider the path loss, i.e. the attenuation of the wave in the conducting medium, and that this decline can be accounted for by using the expression for the attenuation of a plane wave (PW) in a conductive half space. Adopting a slightly less crude approximation, M can be assumed to undergo both the same decay and phase delay experienced by a PW in a conductive half space, and accordingly the mutual inductance would have the complex form

$$M = M_0 \exp[-(1 + \mathrm{j})t/\delta] \tag{1}$$

where M_0 is the mutual inductance in the absence of the conductive medium, whose expression can be found in many textbooks, e.g. [52], t is the thickness of the medium

$$\delta = \sqrt{2/(\omega\sigma\mu)} \tag{2}$$

is the skin depth and μ is the magnetic permeability. As noted in Section 1, this complex M actually corresponds to a coupling impedance with both real and imaginary parts. We shall examine the validity of this approximation, though small magnetic communications terminals and resonators usually operate in the vicinity of conducting interfaces and do not provide a plane magnetic field; moreover, while standard depth of penetration decreases with an increase in conductivity, magnetic permeability or operating frequency, true penetration depth depends also on the conductive material thickness and the selected transmitter parameters. Our starting point is the paper of D&D published some half a century ago [42]. For most of our calculations, we can rely on their quasi-static solution. In that model, a current flows in a thin circular coil at a certain height above a finite conducting slab. Space is divided into four layers (see Fig. 1 in [42]): above the coil, below the coil, but above the conductor, the conductor of finite length and the medium below the conductor. Note that all the media are air with the exception of the conductor. To find an analytical solution in closed form, the authors had to assume that the slab was infinitely wide. They set up a differential equation for the magnetic vector potential and solved it subject to the boundary conditions. The mutual inductance between the transmitting coil and a coil that has the same orientation and is coaxially placed could then be found in terms of the magnetic vector potential $\boldsymbol{A}^{(n)}(r, z)$ in the form

$$M = \frac{2\pi}{S} \int\int_S r\boldsymbol{A}^{(n)}(r, z)\, \mathrm{d}r\, \mathrm{d}z \tag{3}$$

where the superscript (n) refers to the nth layer (the vector potential has different forms in each section), r and z are cylindrical coordinates and S is the area of the receiving coil. The expression for the vector potential is in the form of integrals containing Bessel functions (see the Appendix), and of course, once the vector potential is known over all spaces, the mutual inductance between the transmitting coil and another coil placed anywhere in space can be determined.

3 Determination of the mutual inductance

We need to know how accurate the solution of D&Ds [42] is. Clearly, the conducting medium below the transmitting coil is not infinitely wide. Common sense suggests that if the block has a width somewhat wider than the diameter of the coil that would be sufficient for using the infinitely wide slab assumption. The mutual inductance using again the CST MWS package is plotted for several conductivities in Fig. 4*a* for coils separated by $d = 37$ mm, conducting block thickness $t = 30$ mm and with the transmitting and receiving coils being 22 mm in diameter. The results show that, if the radius of the block is ~4 times larger than the coil radius, then the mutual inductance becomes independent of the block diameter even for the smaller conductivity considered. We have found the mutual inductance by CST MWS also for the case when asymmetry is involved. The conducting medium has again a thickness of 30 mm, but its diameter is fixed at 90 mm. The conductor is initially in the middle of the two coils. Its centre is then moved horizontally in the x-direction by 45 mm in steps of 5 mm. When the plate is moved out of its centre position, then the magnetic field at the lower coil from the upper increases as flux paths around the plate edge shorten. Hence, as the plate moves the mutual inductance will increase. These results are shown in Fig. 4*b*, where the modulus of the mutual inductance is plotted as a function of the horizontal displacement of the conducting block normalised with respect to the distance $(D/2 - r_0)$ between the coil and plate external edges in the original centre-aligned configuration. For low conductivity ($\sigma = 10$), screening is imperfect and M non-zero even at zero offset. The displacement has a more dramatic impact only once and the edge of the plate approaches the perimeter of the coils and conductivity is larger ($\sigma \geq 50$ S/m), which result in M rapidly rising. On the basis of these results, most simulation results presented in the rest of this paper will use a conducting block of size $D = 90$ mm centre-aligned with the pair of coils.

In Fig. 5, we report the mutual inductance calculated for a wide range of block conductivities from 0.01 to 10^4 S/m for the parameters $D = 90$ mm, $d = 37$ mm, $t = 30$ mm, $r_0 = 11$ mm and coil cross-section, $w = 1$ mm. The real part is shown in Fig. 5*a*, the imaginary part in Fig. 5*b*, and the modulus in Fig. 5*c*. There are three curves in each figure showing the three different ways the mutual inductance was determined: by full wave simulations, the PW assumption corresponding to (1), and from the expressions of D&D [42]. There is an excellent agreement between the results of CST MWS and D&D. The curve from the PW assumption (1) is

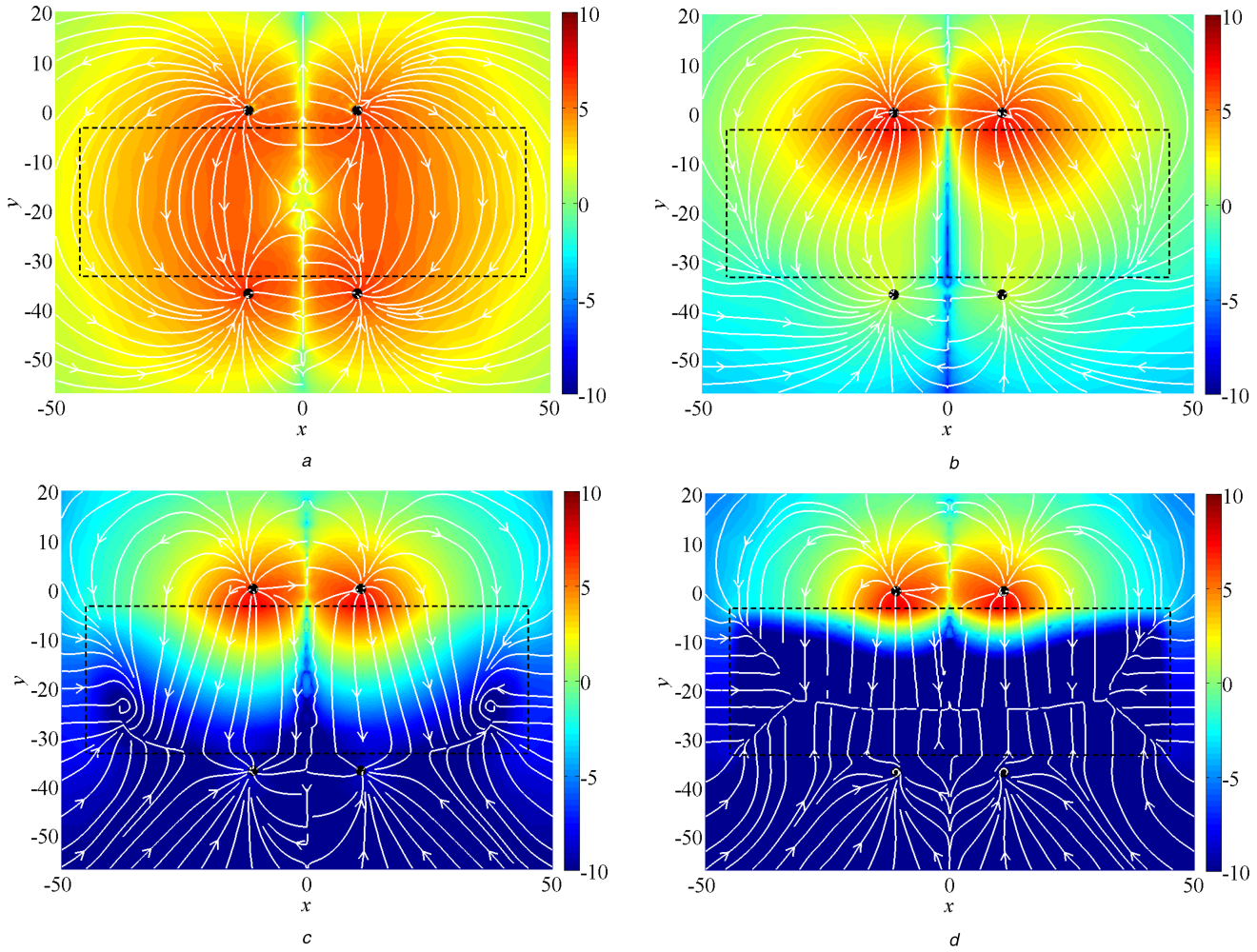

Fig. 3 *Variation of power density from the transmitter to receiver for t = 30 mm, d = 37 mm, f = 159 MHz and* ***(a)*** $\sigma = 0$ S/m, ***(b)*** $\sigma = 10$ S/m, ***(c)*** $\sigma = 10^2$ S/m, ***(d)*** $\sigma = 10^3$ S/m

quite different. As mentioned before, the latter has indeed no theoretical basis. For most applications of coupled coils, the excitation field is not a uniform PW, and so the behaviour of the fields and the eddy currents induced in the conducting block will deviate from the idealised case of a PW. Also, the polarisation of the magnetic field produced by a coil is not that of a PW, as well as its relation to the electric field.

The PW approximation could be applicable when the excitation is a current in a wire or when the current is induced from a very electrically large coil. Indeed, the larger the coil, the more like a uniform PW field the magnetic field will appear to the material. However, for most inductively coupled systems, coils are small and the PW model exhibits large inaccuracy and can only be used for crude approximations of the magnitude of M and the conductivity range over which it decays.

There is one more comment we have to make on the modulus of the mutual inductance. For physical reasons, one would expect M to be a monotonically declining function of conductivity since when conductivity increases the eddy currents increase and hence M modulus must decline. This is indeed the case when the conductor is infinitely wide, as seen in Fig. 5*c*. However, in the case of a finite conductor block, an interference effect also exists between the field contributions that reach the receiving coil through the block and going around it, which is responsible for the small overshoot and undershoot in the magnitude of M predicted by numerical simulations at $\sigma \sim 0.2$ and 80 S/m, respectively.

In Figs. 6*a*–*c*, the mutual inductance is shown as a function of block thickness. As in Fig. 5, three approaches are used: simulations, the analytical solution [42] and the PW approach represented by (1). The curves look similar to those in Fig. 5 in that $|M|$ may again be seen as a monotonically declining function. In fact, an increase in thickness means a larger volume for opposing eddy currents, hence a decline in M modulus follows analogously to the effect produced by the stronger eddy currents associated with larger values of conductivity. Also in these plots, the agreement between the results of CST MWS and D&D is very good, while the PW approximation appears to significantly overestimate attenuation even for small values of the thickness of the conducting block.

4 Experiments

A large number of experiments have been conducted to evaluate the mutual inductance between two coils in the presence of a conducting medium. In our experiments, we measured the transfer function for signals carried between two single turn coils (radius 11 mm) using a vector network analyser (VNA). The conducting medium was placed between them. This was an aqueous solution of sodium chloride with variable concentration placed in a plastic container with dimensions $t = 30$ mm and $D = 90$ mm. The conductivity of sodium chloride solutions was assessed with a conductivity meter, calibrated to a relative accuracy of 2% by using suitable calibration standards. The largest conductivity of the sample solutions used in the experiments was 20 S/m, corresponding to the upper limit of the conductivity meter range.

The measurement setup is shown in Fig. 7*a*, while Fig. 7*b* represents the corresponding CST MWS model used for simulations. The fixture supporting the coils and the container of the conducting solution was placed inside an anechoic chamber to reduce background signals. The coils were arranged in their coaxially aligned positions at the desired spacing distance once and for all at the beginning of the experiments. The container of the conducting solution was realised by three-dimensional printing to have a simple cylindrical shape, as in the simulation model, with

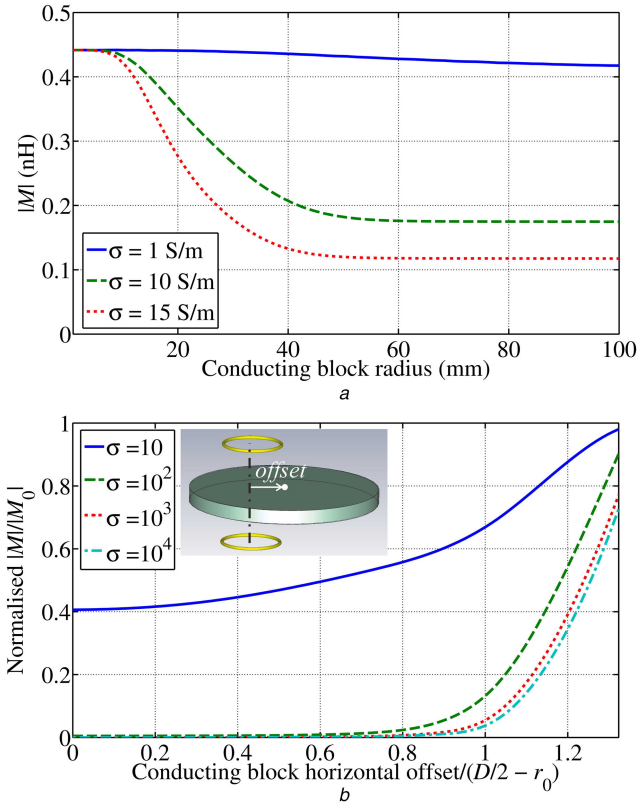

Fig. 4 *Effect of the finite size and position of a 30 mm thick conducting circular plate on the mutual inductance of two coaxially aligned coils separated by d = 37 mm*

(a) $|M|$ as a function of the conducting block diameter for $\sigma = 1$, 10, 15 S/m, ***(b)*** Variation of $|M|$, normalised with respect to the free space value M_0, against the displacement of the conducting circular plate with fixed diameter $D = 90$ mm expressed in terms of the distance of the coil from the edge of the plate. The conductivity of the plate varies from $\sigma = 10$ to 10^4 S/m. Simulations by CST MWS

the upper edge just 2 mm higher than the top surface of the liquid for sliding it in and out of the test fixture to replace the solution without moving the coils.

As according to the block diagram depicted in Fig. 7*c*, the impedance matrix $\mathbf{Z}_{2\text{-port}}$ of the two-port network representing the pair of coils and their coupling through the conducting medium was converted from the scattering parameters obtained from the VNA measurements by de-embedding the effect of the cables and connectors of the measurement fixture. The mutual inductance of the two coupled coils can then be derived by referring to a simple equivalent circuit model of the coils, which under the assumption that the operating frequency is below the coil self-resonance, are simply represented as two coupled inductors, and therefore $Z_{2\text{-port}}$ can be written as

$$Z_{2\text{-port}} = \begin{bmatrix} R + \mathrm{j}\omega L & \mathrm{j}\omega M \\ \mathrm{j}\omega M & R + \mathrm{j}\omega L \end{bmatrix} \tag{4}$$

In the latter expression, R denotes the ohmic resistance of the coils and L and M are generally complex quantities thus corresponding to self- and coupling impedance terms with both real and imaginary parts which take into account the lossy and inductive contributions, respectively, associated with the self- and mutual couplings of the coils in the presence of the conducting block.

In Figs. 8*a–c*, we show the measured mutual inductance (real part, imaginary part and modulus) along with the three sets of theoretical values. In both simulations and the analytical calculations based on the extension of the solution [42] provided in the Appendix, which includes retardation effects and takes into account an arbitrary permittivity of the conducting medium, the dielectric constant of water has been assumed to be $\varepsilon_r = 78$ [53]. Measured M is complex and in good agreement with results of

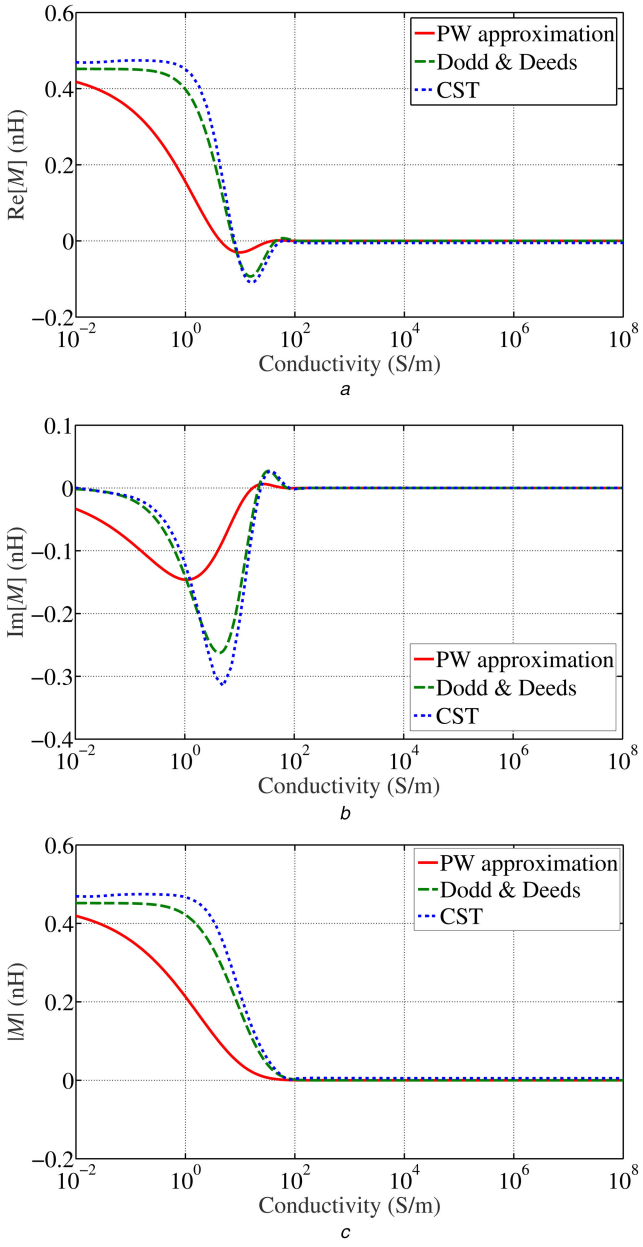

Fig. 5 *Mutual inductance of two coaxially aligned circular coils displaced by d = 37 mm in the presence of a conducting cylindrical block with dimensions D = 90 mm and t = 30 mm as a function of conductivity. Real part*

(a) Imaginary part ***(b)***, Modulus, ***(c)*** Mutual inductance. Simulation results obtained with CST MWS are compared with the analytical solution [42] and PW approximation expressed by (1)

simulations and predictions based on the generalised D&D solution. In particular, the magnitude of measured M falls very close to the values obatined with CST MWS and the generalised D&D formulas, exhibiting practically the same decay. Only for small values of conductivities, i.e. $\sigma < 1$, the analytical results slightly differ from the simulated and measured values: in fact, for vanishing conductivity, the aqueous solution behaves as a high-permittivity dielectric block whose shielding effect more markedly depends on its extension, and correspondingly the mutual inductance exhibits a multi-resonance pattern as a function of variable block radius (this result is omitted due to space limitations); as a result, the infinitely wide slab solution cannot generally provide an accurate model of this situation. However at low frequencies, of interest for inductively coupled systems, conduction effects can overcome dielectric ones already at low conductivity values, even in a medium with large permittivity. This will considerably mitigate the dependence of the coupling between two coils on the actual finite extension of a conducting block.

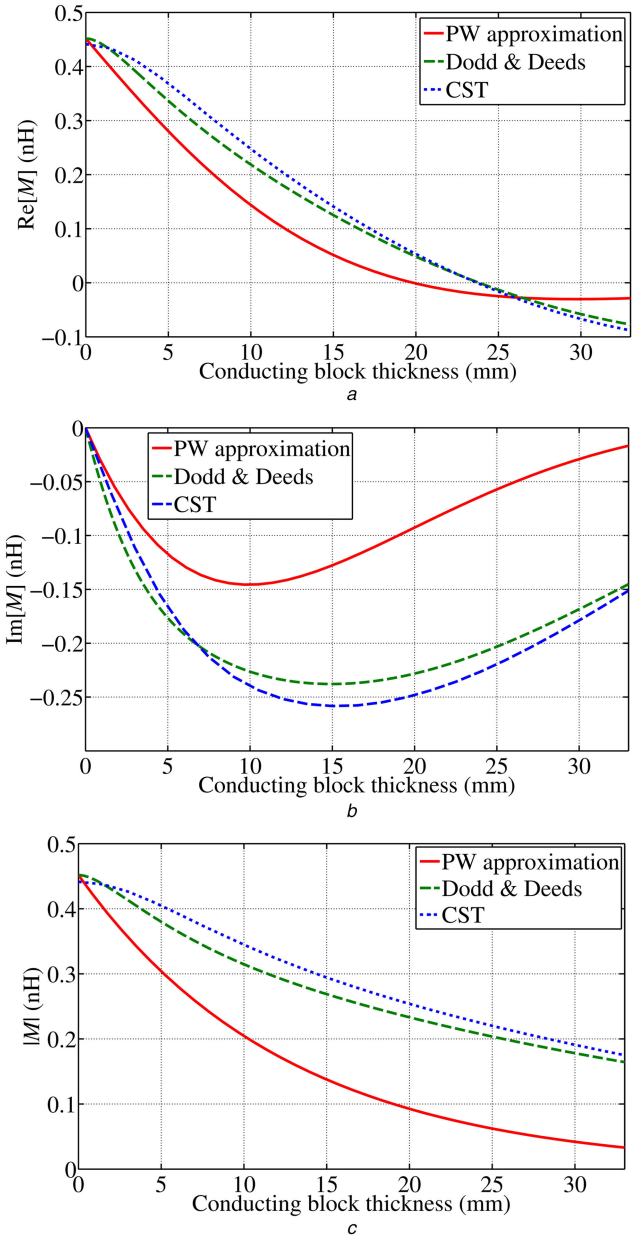

Fig. 6 *Mutual inductance of two coaxially aligned circular coils displaced by 37 mm in the presence of a conducting cylindrical block of conductivity σ = 10 S/m and of width D = 90 mm as a function of thickness*

(a) Real part, ***(b)*** Imaginary part, ***(c)*** Modulus of the mutual inductance. Simulation results obtained with CST MWS are compared with the analytical solution [42] and PW approximation expressed by (1)

Thereby, the dielectric-resonator-like response of a lossy dielectric block and the resonant character of its repercussion on the mutual inductance is restricted to a narrow range of vanishing conductivities, the lower the relative permittivity of the block, the narrower is this range. This trend makes, in turn, the analytical solution for an infinitely wide conducting slab a reliable and accurate tool to predict the impact of a finite conducting block on the mutual inductance of a pair of coils for a broad range of configurations, as previously highlighted in the discussion of Figs. 4–6.

On the other side, it shall be noted that the measured real and imaginary parts of M vanishes and reaches its minimum, respectively, at slightly larger values of conductivity than predicted numerically. These small discrepancies can be attributed to a few factors such as the instrumental precision of the conductivity meter and inaccuracy in VNA calibration, uneven level of the solution due to the surface tension of water, and de-embedding of the effect of measurement cables.

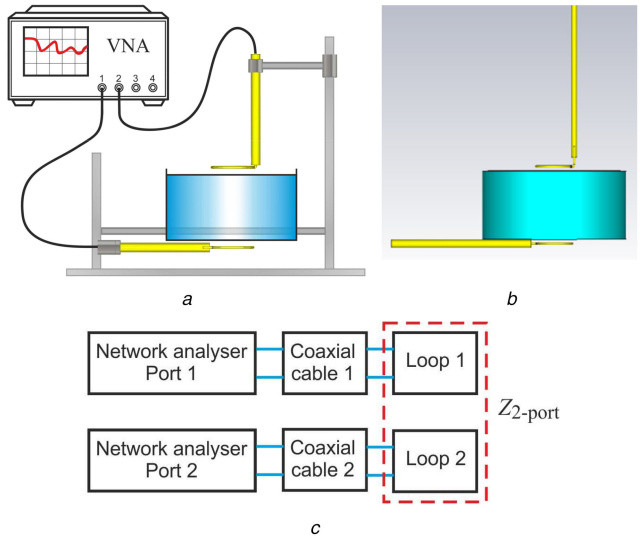

Fig. 7 *Measurement setup*

(a) Schematic view of the measurement set-up, ***(b)*** Corresponding model for simulating the experiments with CST MWS, ***(c)*** Block diagram of the measurement system

It is finally noted that the estimations of the real and imaginary parts of M based on the PW approximation (1) are distant from both simulated and measured values and imply a significant underestimation of the coupling between the coils at the smallest values of conductivity along with a much faster lowering of it than that observed in practise.

5 Conclusions

The amplitude and phase of the mutual inductance between two coils in the presence of a conducting medium have been investigated analytically, experimentally and by simulation. The physics has been illustrated by computing both magnetic field distribution and the state of its polarisation, showing that it is elliptically polarised, and the progress of the Poynting vector from the transmitter to receiver. The results for the mutual inductance (real and imaginary parts) are evaluated for a wide range of medium thicknesses and conductivities. Experiments have been conducted in the range of 0–20 S/m, whereas simulations using the CST numerical package have examined the variation of the mutual inductance over broad variations of all the relevant parameters. In addition, we have assessed the accuracy of a proposal in the literatures [18, 22] that the skin effect expression for attenuation might provide a good estimate. We have found that this is indeed a too simplistic and crude approximation. In particular, predictions based on it of both the real and imaginary parts of the mutual inductance are distant from results obtained by numerical approaches and experiments. The analytical solution [42] generalised in this paper to the arbitrary permittivity of the conducting medium and retardation effects is verified by simulated and experimental data for mutual inductance over a broad range of conductivity and thickness values of an intervening conducting block. Our findings are obviously relevant for the attenuation of MI waves in conducting environment and are also applicable to body area networking and describing properties of biological systems.

6 Acknowledgments

Support for this work was provided by EPSRC Grant EP/N010493/1 as part of the SYMETA project (www.symeta.co.uk). Fruitful discussion with fellow members of the Oxford Metamaterials Network (OxiMETA) are thankfully acknowledged. The Physical and Theoretical Chemistry Laboratory, University of Oxford, is also thanked for providing the conductivity meter for experiments.

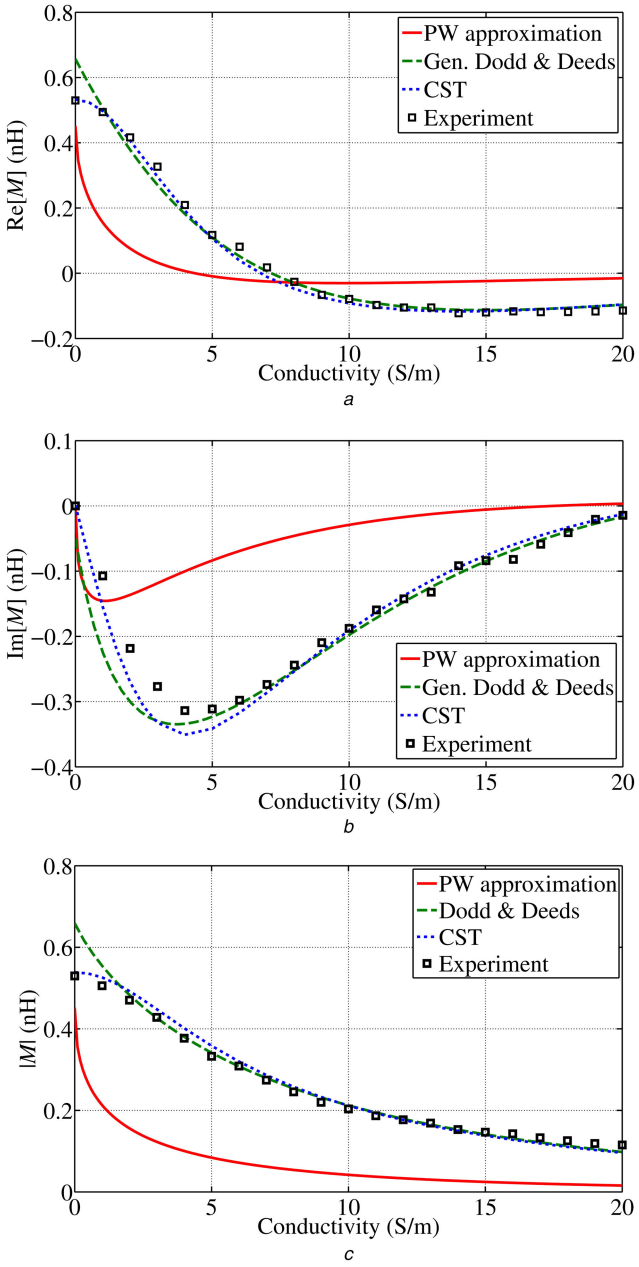

Fig. 8 *Mutual inductance of two coaxial circular coils displaced by 37 mm as a function of conductivity in the presence of a conducting cylindrical block with dimensions D = 90 mm and t = 30 mm*

(a) Measured real, ***(b)*** Imaginary parts, ***(c)*** Modulus. Comparisons are made with results from CST MWS, the analytical solution for an infinitely wide slab [42] generalised to account for retardation effects and the dielectric permittivity of the slab (see the Appendix) and the PW approximation of (1)

7 References

[1] Sojdehei, J., Wrathhall, P., Dinn, D.: 'Magneto-inductive (MI) communications'. MTS/IEEE Conf. Exhibition, OCEANS, Honolulu, Hawaii, November 2001, pp. 5–8

[2] Stevens, C.J., Chan, C.W., Stamatis, K., *et al.*: 'Magnetic metamaterials as 1-D data transfer channels: an application for magneto-inductive waves', *IEEE Trans. Microw. Theory Tech.*, 2010, **58**, (5), pp. 1248–1256

[3] Stevens, C.J.: 'Magnetoinductive waves and wireless power', *IEEE Trans. Power Electron.*, 2015, **30**, (11), pp. 6182–6190

[4] Shamonina, E., Kalinin, V.A., Ringhofer, K.H., *et al.*: 'Magneto-inductive waveguide', *Electron. Lett.*, 2002, **38**, (8), pp. 371–372

[5] Shamonina, E, Kalinin, V.A., Ringhofer, K.H., *et al.*: 'Magnetoinductive waves in one, two, and three dimensions', *J. Appl. Phys.*, 2002, **92**, (10), pp. 6252–6261

[6] Syms, R.R.A., Sydoruk, O., Shamonina, E., *et al.*: 'Higher order interactions in magneto-inductive waveguides', *Metamaterials*, 2007, **1**, pp. 44–51

[7] Zhuromskyy, O., Shamonina, E., Solymar, L.: 'Effect of radiation on dispersion of magneto-inductive waves in a metamaterial', *Proc. SPIE*, 2005, **5955**, pp. 595506-1-595506-7

[8] Wiltshire, M.C.K., Shamonina, E., Young, I.R., *et al.*: 'Experimental and theoretical study of magneto-inductive waves: comparison between theory and experiment', *Electron. Lett.*, 2003, **39**, pp. 215–217

[9] Syms, R.R.A., Young, I.R., Solymar, L.: 'Low-loss magneto-inductive waveguides', *J. Phys. D, Appl. Phys.*, 2006, **39**, pp. 3945–3951

[10] Sydoruk, O., Radkovskaya, A., Zhuromskyy, O., *et al.*: 'Tailoring the near-field guiding properties of magnetic metamaterials with two resonant elements per unit cell', *Phys. Rev. B*, 2006, **73**, pp. 224406-1-224406-12

[11] Radkovskaya, E., Sydoruk, O., Shamonin, M., *et al.*: 'Experimental study of a bi-periodic magnetoinductive waveguide: comparisons with theory', *IET Microw. Antennas Propag.*, 2007, **1**, pp. 80–83

[12] Syms, R.R.A., Solymar, L., Young, I. R., *et al.*: 'Thin film magneto-inductive cables', *J. Phys. D, Appl. Phys.*, 2010, **43**, pp. 055102-1-055102-7

[13] Syms, R.R.A., Shamonina, E., Solymar, L.: 'Magnetoinductive waveguide devices', *IEE Proc. Microw. Antennas Propag.*, 2006, **153**, (2), pp. 111–121

[14] Akyildiz, I.F., Stuntebeck, E.P.: 'Wireless underground sensor networks: research challenges', *Ad Hoc Netw.*, 2006, **4**, pp. 669–686

[15] Sun, Z., Akyildiz, I.F.: 'Underground wireless communication using magnetic induction'. 2009 IEEE Int. Conf. Communications, Dresden, 2009, pp. 1–5

[16] Syms, R.R.A., Solymar, L.: 'Noise in metamaterials', *J. Appl. Phys.*, 2011, **109**, pp. 124909-1–124909-5

[17] Sun, Z., Akyildiz, I.F.: 'Magnetic induction communications for wireless underground sensor networks', *IEEE Trans. Antennas Propag.*, 2010, **58**, (7), pp. 2427–2435

[18] Kisseleff, S., Sun, Z., Akyildiz, I.F.: 'Channel capacity of magnetic induction based wireless underground sensor networks under practical constraints'. 2013 IEEE Wireless Communications and Networking Conf. (WCNC), Shanghai, Shanghai, China, 2013, pp. 2603–2608

[19] Sun, Z., Akyildiz, I.F., Kisseleff, S., *et al.*: 'Increasing the capacity of magnetic induction communications in RF-challenged environments', *IEEE Trans. Commun.*, 2013, **61**, (9), pp. 3943–3952

[20] Kisseleff, S., Akyildiz, I.F., Gerstacker, W.H.: 'Digital signal transmission in magnetic induction based wireless underground sensor networks', *IEEE Trans. Commun.*, 2015, **63**, (6), pp. 2300–2311

[21] Kisseleff, S., Akyildiz, I.F., Gerstacker, W.H.: 'Throughput of the magnetic induction based wireless underground sensor networks: key optimisation techniques', *IEEE Trans. Commun.*, 2014, **62**, (12), pp. 4426–4439

[22] Ma, J., Zhang, X., Huang, Q., *et al.*: 'Experimental study of the impact of soil conductivity on underground magneto-inductive channel', *IEEE Antennas Wirel. Propag. Lett.*, 2015, **14**, pp. 1782–1785

[23] Gulbahar, B., Akan, O.B.: 'A communication theoretical modelling and analysis of underwater magneto-inductive wireless channels', *IEEE Trans. Wirel. Commun.*, 2012, **11**, (9), pp. 3326–3334

[24] Akyildiz, I.F., Wang, P., Sun, Z.: 'Realizing underwater communication through magnetic induction', *IEEE Commun. Mag.*, 2015, **53**, (11), pp. 42–48

[25] Sun, Z., Wang, P., Vuran, M.C., *et al.*: ' MISE-PIPE: magnetic induction-based wireless sensor networks for underground pipeline monitoring', *Ad Hoc Netw.*, 2011, **9**, pp. 218–227

[26] Nitz, W.R., Oppelt, A., Renz, W., *et al.*: 'On the heating of linear conductive structures as guide wires and catheters in interventional MRI', *J. Magn. Reson. Imaging*, 2001, **13**, (1), pp. 105–114

[27] Syms, R.R.A., Young, I.R., Ahmad, M.M., *et al.*: 'Magneto-inductive catheter receiver for magnetic resonance imaging', *IEEE Trans. Biomed. Eng.*, 2013, **60**, (9), pp. 2421–2431

[28] Syms, R.R.A., Young, I.R., Rea, M.: 'Frequency scaling of catheter-based magneto-inductive MR imaging detectors'. Proc. 17th Int. Conf. Solid State Sensors Actuators Microsystems Transducers, Eurosensors, Barcelona, June 2013, pp. 594–597

[29] Kardoulaki, E.M., Syms, R.R.A., Young, I.R., *et al.*: 'SNR on MI catheter receivers FPR MRI', *IEEE Sens. J.*, 2016, **16**, (6), pp. 1700–1707

[30] Doll, H.G.: 'Introduction to induction logging and application to logging of wells drilled with oil base mud', *J. Pet. Technol.*, 1949, **1**, (6), pp. 148–162

[31] Dusterhoeft, Jr.W.C., Smith, H.W.: 'Propagation effects on radial response in induction logging', *Geophysics*, 1962, **27**, pp. 463–469

[32] Moran, J.H., Kunz, K.S.: 'Geophysics: basic theory of induction logging and application to study of two-coil sondes', *Geophysics*, 1962, **27**, pp. 829–859

[33] Wait, J.R.: 'General formulation of the induction logging problem for concentric layers about the bore hole', *IEEE Trans. Geosci. Remote Sens.*, 1984, **22**, (1), pp. 34–42

[34] Kaufman, A.A., Dashevsky, Y.A.: '*Principles of induction logging*' (Elsevier, Amsterdam, The Netherlands, 2003)

[35] Tesla, N.: 'The transmission of electric energy without wires', *Electr. World Eng.*, 1904, **5**, pp. 162–167

[36] Tesla, N.: 'The transmission of electrical energy without wires as a means of furthering peace', *Electr. World Eng.*, 1905, **45**, (1), pp. 21–24

[37] Urzhumov, Y., Smith, D.R.: 'Metamaterial-enhanced coupling between magnetic dipoles for efficient wireless power transfer', *Phys. Rev. B*, 2011, **83**, (20), pp. 205114-1-205114-5

[38] Stevens, C.J.: 'Power transfer via metamaterials', *Comput. Mater. Continua*, 2013, **33**, (1), pp. 1–18

[39] Levy, S.: 'Electromagnetic shielding effect of an infinite plane conducting sheet placed between circular coaxial coils', *Proc. IRE*, 1936, **24**, pp. 923–941

[40] Smythe, W.R.: '*Static and dynamic electricity*' (McGraw-Hill, New York, 1950)

[41] Foggo, S.M., Norris, W.T., Thomas, D.I.: 'The shielding effect of a plane conducting sheet between two coaxial coils', *J. Phys. D*, 1969, **2**, pp. 1599–1607

[42] Dodd, C.V., Deeds, W.E.: 'Analytical solutions to eddy current coil problems', *J. Appl. Phys.*, 1968, **39**, pp. 2829–2838

[43] Burke, S.K., Ibrahim, M.E.: 'Mutual impedance of air-cored coils above a conducting plate', *J. Phys. D, Appl. Phys.*, 2004, **37**, pp. 1857–1868

[44] Teodoulidis, T.P., Ditchburn, R.J.: 'Mutual impedance of cylindrical coils at an arbitrary position and orientation above a planar conductor', *IEEE Trans. Magn.*, 2007, **43**, (8), pp. 3368–3370
[45] Hurley, W.G., Duffy, M.C.: 'Calculation of self and mutual impedances in planar magnetic structures', *IEEE Trans. Magn.*, 1995, **31**, (4), pp. 2416–2422
[46] Su, Y.P., Liu, X., Hui, S.Y.R.: 'Mutual inductance calculation of movable planar coils on parallel surfaces', *IEEE Trans. Power Electron.*, 2009, **24**, (4), pp. 1115–1123
[47] Carretero, C., Alonso, R., Acero, J., *et al.*: 'Coupling impedance between planar coils inside a layered media', *Prog. Electromagn. Res.*, 2011, **112**, pp. 381–396
[48] Acero, J., Carretero, C., Lope, I., *et al.*: 'Analysis of the mutual inductance of planar-lumped inductive power transfer systems', *IEEE Trans. Ind. Electron.*, 2013, **60**, (1), pp. 410–420
[49] Cao, B., Li, C., Fan, M., *et al.*: 'Analytical modelling of eddy current response from driver pick-up coils on multi-layered conducting plates', *Insight, Non-Destr. Test. Cond. Monit.*, 2018, **60**, (2), pp. 77–83
[50] Vallecchi, A., Chu, S., Stevens, C.J., *et al.*: 'Impact of a conducting medium on the coupling of meta-atoms'. Tenth Int. Congress on Advanced Electromagnetic Materials in Microwave and Optics – Metamaterials 2016, Crete, Greece, 17–22 September 2016
[51] CST Microwave Studio, User Manual, 2017
[52] Paul, C.R.: '*Inductance: loop and partial*' (John Wiley & Sons, Hoboken, New Jersey, 2011)
[53] Komarov, V., Wang, S., Tang, J.: 'Permittivity and measurements', in Chang, K., (Ed.): '*Encyclopedia of RF and microwave engineering*' (John Wiley & Sons, Inc., Hoboken, New Jersey, 2005), pp. 3693–3711

8 Appendix. D&Ds' solution for a coil above a conducting slab including retardation effects

For our calculations, we shall use a geometry that is a special case of that considered by D&Ds [42] in the sense that the medium below the conductor is taken as air. Moreover, we will assume that the conducting slab has an arbitrary permittivity ε_r. Analogously to [42], the solution can be expressed in terms of the magnetic vector potential that, due to the axial symmetry, has only a single component along the azimuthal angle ϕ, i.e. $\boldsymbol{A} = A_\phi(r, z)\hat{\boldsymbol{\phi}}$. D&Ds then find the vector potential in the form of integrals containing first-order Bessel functions. Expressions, obtained by generalising D&Ds' formulae to include retardation, are given below:

$$A_\phi^i = A_\phi^i(r, z) = \mu_0 I_0 r_0 \int_0^\infty J_1(\alpha r_0) J_1(\alpha r) F_i(\alpha, z)\alpha \, \mathrm{d}\alpha \tag{5}$$

where the index i, $i = 1, 2, 3, 4$ refers to the different regions in which the problem is divided, i.e. above the coil ($i = 1$), below the coil, but above the conductor ($i = 2$), the conductor of finite length ($i = 3$), the medium below the conductor ($i = 4$) and the spectral functions $F_i(\alpha, z)$, obtained by imposing the continuity of the electric and magnetic fields at the various interfaces, are:

$$\begin{aligned}
F_1 &= \frac{\mathrm{e}^{-\alpha_0(z-l)}}{2\alpha_0} + \frac{(\alpha_0-\alpha_1)(\alpha_0+\alpha_1)\left(\mathrm{e}^{2\alpha_1 t}-1\right)}{(\alpha_0+\alpha_1)^2\mathrm{e}^{2\alpha_1 t}-(\alpha_0-\alpha_1)^2}\frac{\mathrm{e}^{-\alpha_0(z+l)}}{2\alpha_0} \\
F_2 &= \frac{\mathrm{e}^{-\alpha_0(l-z)}}{2\alpha_0} + \frac{(\alpha_0-\alpha_1)(\alpha_0+\alpha_1)\left(\mathrm{e}^{2\alpha_1 t}-1\right)}{(\alpha_0+\alpha_1)^2\mathrm{e}^{2\alpha_1 t}-(\alpha_0-\alpha_1)^2}\frac{\mathrm{e}^{-\alpha_0(l+z)}}{2\alpha_0} \\
F_3 &= \mathrm{e}^{-\alpha_0 l}\frac{(\alpha_0+\alpha_1)\mathrm{e}^{2\alpha_1 t}\mathrm{e}^{\alpha_1 z}+(\alpha_1-\alpha_0)\mathrm{e}^{-\alpha_1 z}}{(\alpha_0+\alpha_1)^2\mathrm{e}^{2\alpha_1 t}-(\alpha_0-\alpha_1)^2} \\
F_4 &= \mathrm{e}^{-\alpha_0 l}\frac{2\alpha_1\mathrm{e}^{(\alpha_0+\alpha_1)t}\mathrm{e}^{\alpha_0 z}}{(\alpha_0+\alpha_1)^2\mathrm{e}^{2\alpha_1 t}-(\alpha_0-\alpha_1)^2}
\end{aligned} \tag{6}$$

In (6), $z = l$ correspond to the position of the coil above the conducting slab, whose upper face is assumed to be located at $z = 0$; moreover, α_0 and α_1 are the quantities introduced in the derivation of the solution by the method of separation of variables that are related to the permittivity, permeability and conductivity of the different regions

$$\begin{aligned}
\alpha_0 &= \sqrt{\alpha^2 - \omega^2\mu_0\varepsilon_0}, \\
\alpha_1 &= \sqrt{\alpha^2 - \omega^2\mu_0\varepsilon_0\varepsilon_r + \mathrm{j}\omega\mu_0\sigma_1}
\end{aligned} \tag{7}$$

The differences from D&Ds' quasi-static solution appear as in [42] the assumption is made that the term $\omega^2\mu_0\varepsilon_0$ in (7) is negligible and, therefore, it is taken $\alpha_0 \simeq \alpha$ and $\alpha_1 \simeq \sqrt{\alpha^2 + \mathrm{j}\omega\mu_0\sigma_1}$. The use of (7) in (5) and (6) retains in the solution the effects of retardation and takes into account an arbitrary permittivity of the conducting medium. While this generalisation of D&D's analysis obviously reduces to the original magneto-quasi-static approximation as long as $\omega^2\mu_0\varepsilon_0 \to 0$ and $\omega\varepsilon_0\varepsilon_r \ll \sigma_1$, when these conditions have not fulfilled the solution in [42] can lead to substantial inaccuracies in the prediction of the mutual inductance. This is the case, for example, of the experiments described in Section 4, for which at $\omega = 10^9$ rad/s and for $\varepsilon_r = 78$ its results $\omega\varepsilon_0\varepsilon_r \cong 0.7$, implying that the magneto-quasi-static solution would not be applicable roughly for $\sigma_1 \leq 10$. It is also worth noting that, based on the analyses we performed, the computational effort involved in the calculation of D&Ds' solution [42] or its generalisation are substantially similar. Therefore, unless the criteria recalled above are strictly verified, for a more precise estimation of M it can be advantageous to resort to the complete solution including dielectric and retardation effects. Finally, it is worth noting that another situation in which retardation could matter is when the structure under consideration is electrically large, e.g. when there is an array with a total length larger than the wavelength, in which case the coupling between distant coils should be calculated by the generalised solution for M.